



Parametric study of nonlinear finite element punching behavior of fiber-reinforced concrete slab

Fiber takviyeli beton döşemenin doğrusal olmayan zımbalama davranışı üzerine parametrik bir çalışma

Mohammed S. Al Jawahery¹ , Mehmet Tolga Göğüş^{2,*} , Rayan Faiz Hadi Boto³ 

¹ Architecture Engineering Department, College of Engineering, University of Mosul, 41001 Mosul, Iraq

² Gaziantep University, Civil Engineering Department, 27310, Gaziantep, Türkiye

³ Gaziantep University, Graduate School of Natural & Applied Sciences, 27310, Gaziantep, Türkiye

Abstract

This paper investigates the effect of fiber on the behavior of punching shear slabs; a finite element modeling approach is used to simulate the case study. The proportion mix of hybrid fiber-reinforced concrete, which contains 0.2 percent macro synthetic fibers and 0.68, 0.8, and 0.96 percent steel fibers, compressive strengths of 50 MPa, different longitudinal reinforcement used, and slab thicknesses of 150, 200, and 250 mm are all joined and investigated in this study. The ATENA software is used to perform nonlinear finite element analysis. The slab results validation was done similarly to previous experimental work, and the acquired results indicated a significant agreement. Thirty-six two-way specimen slabs with dimensions of 1900 × 1900mm were modeled in this investigation. All four sides of the slabs are supported. The results showed that the slabs' ultimate shear capacity increases with increasing the hybrid steel fiber. Nevertheless, the ultimate capacity of the slabs has decreased due to an increase in the reinforcement ratio and slab thickness.

Keywords: Slabs, HFRC slabs, Finite element method, Nonlinear analysis

1 Introduction

Slabs are the prominent structural members in any multi-story structure; it directly carries the live load [1]. When a slab has been supported directly on columns without beams, a flat slab knows it [2]; therefore, the punching shear stresses generated near the columns primarily control the flat plate depth [3]. To keep the thickness of the slab as low as possible and to prevent the column from disastrously failing and brittle failure by "punching" through the slab, the designer's responsibility should be to decrease shear stress at the slab column edge or to increase shear resistance at the slab column edge [4, 5].

Fiber Reinforced Concrete (FRC) is a concrete mix containing various fibrous materials to improve structural strength and durability [6]. Fibers are widely used in concrete to prevent cracking caused by both plastic and drying shrinkage. Polypropylene, glass, and steel fibers are

Öz

Bu makale, döşemelerin zımbalama kesmesi davranışı üzerinde lifin etkisini araştırmaktadır; vaka çalışmasını simüle etmek için bir sonlu eleman modelleme yaklaşımı kullanılmıştır. Yüzde 0.2 makro sentetik lifler ve yüzde 0.68, 0.8 ve 0.96 çelik lifler, 50 MPa basınç dayanımları, kullanılan farklı boyuna donatılar ve 150, 200 ve 250 mm levha kalınlıkları içeren hibrid lif takviyeli betonun oranı karışımı hepsi bu çalışmada birleştirilmiş ve incelenmiştir. ATENA yazılım doğrusal olmayan sonlu eleman analizi yapmak için kullanılmıştır. Döşeme sonuçlarının doğrulanması, önceki deneysel çalışmalara benzer şekilde yapıldı ve elde edilen sonuçlar, büyük bir yakınlığın bulunduğunu gösterdi. Bu araştırmada, 1900 × 1900 mm boyutlarında otuz altı adet çift yönlü döşeme numunesi modellenmiştir. Döşemelerin dört tarafı da basit mesnetlidir. Sonuçlar, hibrit çelik elyaf ile döşemelerin nihai kesme kapasitesinin arttığını göstermiştir. Bununla birlikte, takviye oranındaki ve plaka kalınlığındaki artış nedeniyle plakaların nihai kapasitesi azalmıştır.

Anahtar kelimeler: Döşemeler, HFRC döşemeler, Sonlu Elemanlar Metodu, Doğrusal olmayan analiz.

some of concrete's most commonly used fibers. A hybrid fiber reinforced concrete is a concrete composite containing two or more fibers [7, 8]. Combining metallic and non-metallic fibers has been shown to improve the properties of concrete substantially. The ruling to combine two fibers can be based on their individual properties or simply on cost. Mixing steel with polypropylene fibers resulted in a significant rise in load-deflection response [9, 10]. Steel fibers for concrete reinforcement are defined as tiny, discrete lengths of steel with a volume fraction of 20 to 100, several cross-sections, and small enough to be distributed uniformly in an unhardened concrete mixture using standard mixing techniques [11]. Synthetic fibers are kid fibers that are the products of petrochemical and textile industry research and development [12]. On the other hand, synthetic fibres are useful in the early stages of a composite's existence, where the matrix is weak, brittle, and has a low modulus. Improved

* Sorumlu yazar / Corresponding author, e-posta / e-mail: mtgogus@gantep.edu.tr (M. T. Göğüş)

Geliş / Recieved: 17.08.2021 Kabul / Accepted: 22.09.2023 Yayınlanma / Published: 15.10.2023

doi: 10.28948/ngmuh.983719

material hardness in mature concrete is based on fiber volume value and fiber strength in the matrix [13].

Punching shear is a case of brittle failure after a concentrated force is supplied to a slab [14]. Many factors influence the punching shear strength of flat slabs. The compressive strength of concrete f_c' is one of the most significant. The effect occurs directly or indirectly while concrete tensile strength f_{ct} is used. The second parameter is the geometrical ratio of the longitudinal reinforcement; a third important parameter is d (instead of h , which is the overall slab height): a more significant depth improves the punching shear and the flexural strength of the slab [5, 15]. Punching defects in concrete are caused by low tensile strength, stiffness, flexural strength, shear strength, and brittleness [16]. However, punching failure is one of the most common failure mechanisms for this kind of structural system, it happened suddenly, with catastrophic results. In addition, without any warning [17].

(AlHamaydeh and Anwar Orabi, 2021) examined the behavior of synthetic fiber-reinforced to improve the shear capacity of flat slabs that were reinforced by employing glass fiber-reinforced polymer bars. Their findings can be found in the article. Six large-scale slabs are a part of the experimental program. According to the findings of the investigation, the punching shear resistances were only slightly improved when the synthetic fiber was utilized instead of the control slabs, and the result was an increase in toughness that was 2.34 times greater on average [18].

This study examines the influence of hybrid fiber on the behavior of punching shear flat slabs; a finite element modeling approach is used to simulate the case study. several parameters entered and examined in this study; the proportion mix of hybrid fibre-reinforced concrete, compressive strength, the ratio of the longitudinal reinforcement, and thickness of slabs.

2 Finite element modeling of hybrid fiber-reinforced concrete slab

2.1 General

Finite element analysis is a numerical method used by engineers to solve various challenges. One of the method's basic assumptions is that the domain may be partitioned into smaller parts where the equations may be approximated and solved. The region can also be partitioned into a finite number of elements linked together via nodes. The behavior of all structures may be represented by assembling the solution for each region [19].

To ensure the accuracy of the model used in the punching shear simulations in reinforced concrete, simulations had run and the results were compared to experimental data. Eight test specimens were simulated in this study, and the experimental findings should be compared to the data from the finite element calculations [17, 20].

Based on the experimental study [17], two of the experiment's test specimens were simulated using ATENA. The first simulation involved four-test prism specimens, one as a reference and the other three with varying numbers of fibers, so the dimensions of the prism were 100×100

×400mm according to the ASTM 1609/C1609M-05 standard to simulate the flexural strength of the HFRC.

The other simulated specimens were eight full-scale two-way slabs with dimensions of 1900×1900mm and 200 and 250mm thicknesses with various volume fibers. The slabs were loaded centrally using a 250×250mm column stub. The slabs were simply supported along all four sides. It is classified into two groups with 150, 200 and 250mm thicknesses. Each group had a varied percentage of fiber volume fractions of 0, 0.68, 0.8, and 0.96%. The fiber volume fraction was set at 0% in the reference slabs. The specimens were made with hooked-type steel fibers, and the synthetic fibers used in this study had a 90 aspect ratio. The manufacturer's specifications for the fibers used are presented in Table 1 [17].

2.2 Finite element modeling

For finite element analysis of punching shear in slabs, the software packages ATENA and GiD 3D were utilized [20]. The data preparation and mesh creation of models were done with GiD, while the FE analysis was done with ATENA. Cervenka Consulting has developed ATENA, a nonlinear finite element-based program for the study of RC-Structures The Fracture-plastic model was used in this study to combine constitutive models for tensile (fracturing) and compressive (plastic) behavior. The fracture model is based on the orthotropic smeared crack formulation and the crack band concept. The bilinear law, elastic-perfectly plastic model is used in this study as a constitutive model of steel reinforcement, The concrete was modeled using 3D solid hexahedron (brick) components with 8 nodes (CCIsoBrick<xxxxxxx>) with CC3DnonLin Cementitious2User material that is suitable for rock or concrete like materials. The steel reinforcing bars were modeled using 3D truss elements with 3 nodes (CCIsoTruss<xxx>) with CCReinforcement material, it can be used to define the material parameters for bars or tendons based on the reinforcement steel strength class, more information can be found out in the manual of Atena [21-24].

To allow for a reduction in the required computer capacity, it was comfortable and acceptable to simulate only a quarter of the test specimens due to symmetry [20]. In the symmetries, boundary conditions were used to prevent free movement in the direction of geometrical continuity. The FE model's geometry is constructed, also material properties were assigned to the various elements of the HFRC slab specimen; support, loading conditions, monitoring points, reinforcement details, and mesh in the HFRC slab are all described in Figure 1.

2.3 Parametric study of HFRC slabs

The parameters examined in this paper are the slab thickness, the strength of concrete, and the reinforcement ratio for the HFRC slab with a variant proportion of fibers. The dimensions of the slabs are 1900×1900mm with thicknesses of 150, 200, and 250mm. This study also covered the compressive strength utilized, 50MPa, to investigate the punching behavior of the HFRC slab. In addition, three types of steel bars were utilized in this study to explore the effect of the reinforcement ratio. The steel bar diameter in the

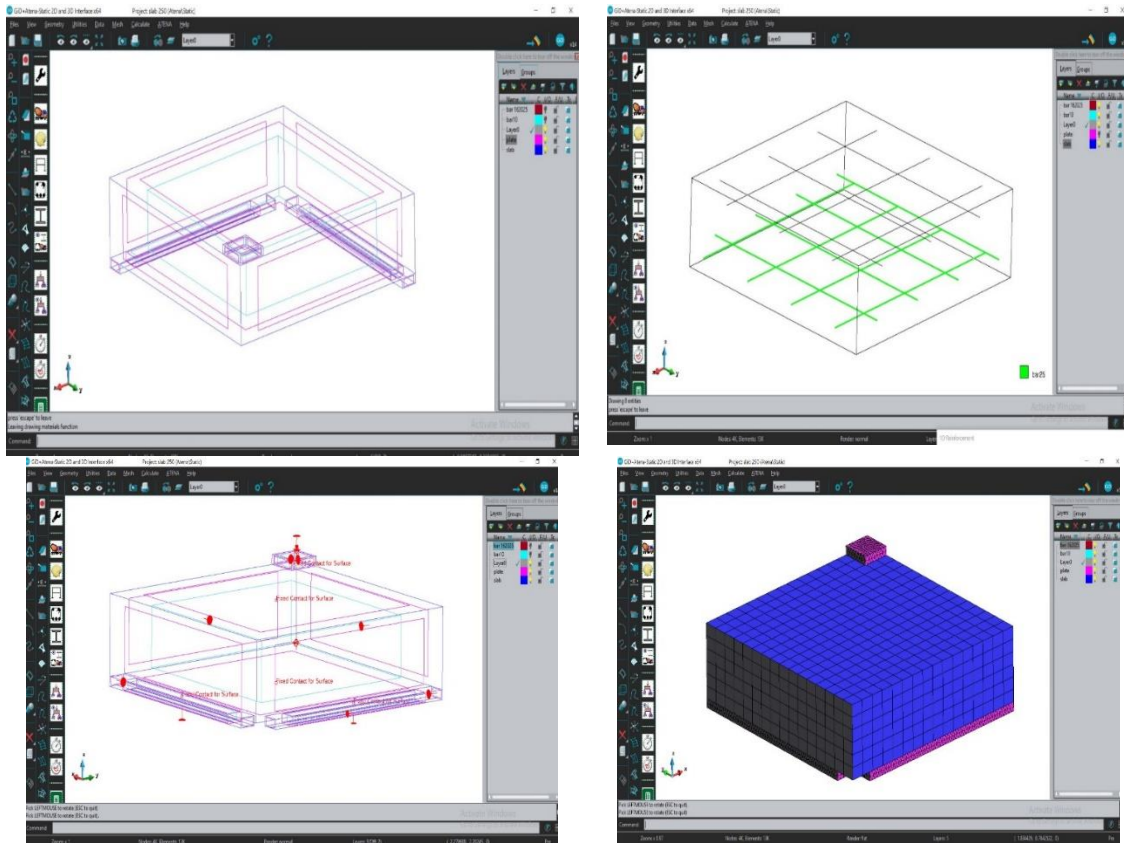


Figure 1. Display FE model's geometry with support, loading conditions, monitoring points, reinforcement details, and mesh in the HFRC slab

Table 1. Displays the prism results of ultimate load and deflection for experimental and FE models.

Steel fibers	Fiber type	-	Hooked
	Fiber length	L_f (mm)	50
	Fiber diameter	D_f (mm)	1.1
	Ultimate tensile strength	MPa	1100
Macro synthetic fibers	Fiber length	L_f (mm)	40
	Fiber diameter	D_f (mm)	0.45
	Ultimate tensile strength	MPa	620

bottom layer was 16 mm, 20 mm, and 25 mm, with reinforcement ratios (A_s/A_c) of 0.54, 0.84, and 1.31% for 150mm thickness, 0.4, 0.63, and 0.98% for 200mm thickness, and 0.32, 0.5, and 0.79% for 250mm thickness, respectively. The top layer of the steel bar was similar in all specimens about 10 mm.

3 Results and discussions

3.1 Validation results of HFRC flexural strength

The experimental and FE model results for four prisms, one as a reference and the others with varying fiber volume, are shown in Table 2. Furthermore, the load-deflection curves of prisms for experimental and FE model results for ultimate load capacity (P) and deflection at ultimate loads (Δ) of HFRC flexural strength are shown in Figures 2 and 3.

The FE model's results were close to the experimental study's results, as shown in Table 2, Figure 2, and Figure 3.

Therefore, the flexural strength results can be utilized to simulate HFRC slab specimens in the following steps.

3.2 Validation results of HFRC slabs

In this investigation, eight test specimens were simulated, with four specimens of 200 mm thickness and four specimens of 250 mm thickness, the experimental results were compared to simulations of finite element data. For each slab thickness, two specimens were chosen as a reference, while the remaining six specimens had varying volume fibers. Table 3, and 4 displays the specimen findings for ultimate load and deflection for experimental and FE models for HFRC slabs of 200 mm and 250 mm thickness.

As a result, Figures 4 and 5 show the load-deflection curves of the HFRC slab with a thickness of 200mm for the Exp. and FE models. Furthermore, Figures 6 and 7 show the load-deflection curves of the HFRC slab with a thickness of 250 mm for the Exp. and FE models.

Table 2. Displays the prism results of ultimate load and deflection for experimental and FE models.

No.	Prism type	Experimental		Finite Element	
		$P_{exp.}$ (KN)	$\Delta_{exp.}$ (mm)	P_{ATENA} (KN)	Δ_{ATENA} (mm)
1	Reference	14.3	0.66	14.25	0.01
2	HFR-0.68/0.2	18.64	0.7	18.75	0.65
3	HFR-0.80/0.2	18.89	0.67	18.93	0.93
4	HFR-0.96/0.2	21.91	1.34	22.31	1.22

Table 3. Displays the slab results of ultimate load and deflection for experimental and FE models.

No.	Specimens name	Experimental		Finite Element	
		$P_{exp.}$ (KN)	$\Delta_{exp.}$ (mm)	P_{ATENA} (KN)	Δ_{ATENA} (mm)
1	Reference 200	847.9	19.91	863.15	10.65
2	HFR200-0.68/0.2	978.1	21.23	1008.69	11.2
3	HFR200-0.80/0.2	1029.9	16.97	1014.63	14.95
4	HFR200-0.96/0.2	1117.6	19.97	1100.32	16.43
5	Reference 250	1147.6	11.66	1143.01	6.17
6	HFR250-0.68/0.2	1375.5	15.19	1336.8	8.12
7	HFR250-0.80/0.2	1300.2	14.12	1350.38	8.3
8	HFR250-0.96/0.2	1386.5	15.97	1486.68	9.46

The ultimate load and deflection calculated for the experimental and numerical models had reviewed in Table 3, when comparing them, distinguish that the ultimate load values were close to the experimental value. Nevertheless, the deflection values were acceptable when compared to experimental data. It is possible to say that the numerically obtained results are accurate compared to the experimentally obtained results.

In addition, Table 4 shows the experimental cracking pattern and finite element-cracking pattern for each slab of 200 mm and 250 mm HFR. When compared to crack pattern failure in experimental and finite elements, the numerical failure appears to have been accurate for the experimental failure.

3.3 Parametric result of HFRc slabs

Reinforcement ratio and slab thickness were the main variables in this paper. For determining the effects of the fiber volume percentage on each slab specimen. Therefore, 36 specimen models had classified into three groups based on slab thickness 150, 200, and 250 mm. Each HFRc slab group has 12 models classified by reinforcement ratio (ρ), slab thickness (h), and fibers volume (V_f).

The ultimate load and deflection results are presented in Table 4. In addition, Table 5 displays the load-deflection curves with a Finite Element crack pattern for all groups. It is clear to see that each parameter has a distinct influence on the shear capacity of the material. In addition, the effective values that can offer a more desirable value of ultimate shear strength are $f_c' = 90\text{MPa}$, $h = 150\text{ mm}$, steel reinforcement ratio $= 0.54\%$, and steel fiber ratio $= 0.96\%$. These values are all comprised of steel. The combination of these findings lends some credence to the conceptual premise that an increase in compressive strength results in an increase in shear capacity; however, the mean improvement in high compressive strength is dependent on the variation of

compressive strength, and it is more active when it changes from 50 to 70 MPa than when it changes from 70 until it reaches 90 MPa. This indicates that if the designer is looking for a value of compressive strength that is both more active and economical, the choice will be 70 MPa rather than 90 MPa, the thickness will be 150 mm, 0.54% of steel reinforcement ratio as well as 0.96% of steel fiber ratio will give the best results of shear capacity, and the ratio of steel fiber to steel reinforcement will be 0.96%.

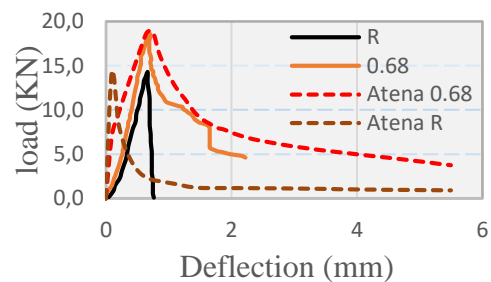


Figure 2. Displays the load-deflection curves of prisms for Experimental and FE models for reference and HFRc-0.68/0.2

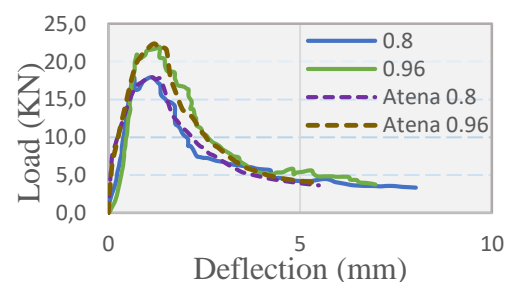


Figure 3. Displays the load-deflection curves of prisms for Experimental and FE models for HFRc-0.8/0.2 and HFRc-0.96/0.2

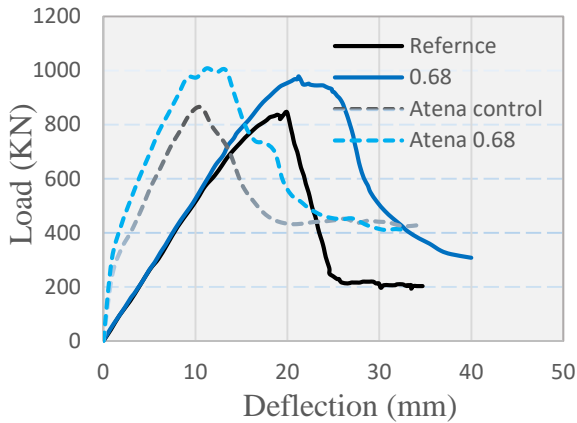


Figure 4. Displays the load-deflection curves of HFRC slab 200mm for Exp. and FE models for reference200 and HFR200-0.68/0.2

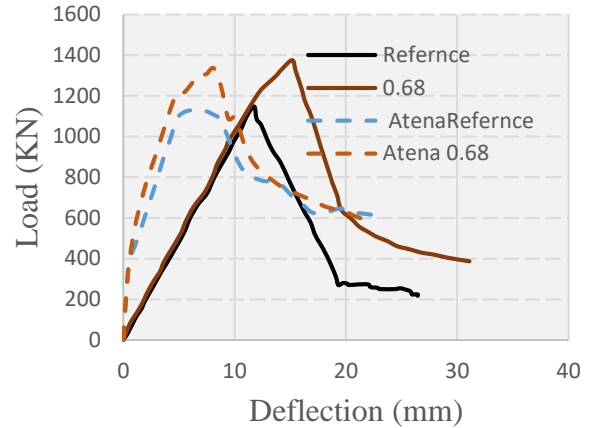


Figure 6. Displays the load-deflection curves of HFRC slab 250mm for Exp. and FE models for reference250 and HFR250-0.68/0.2

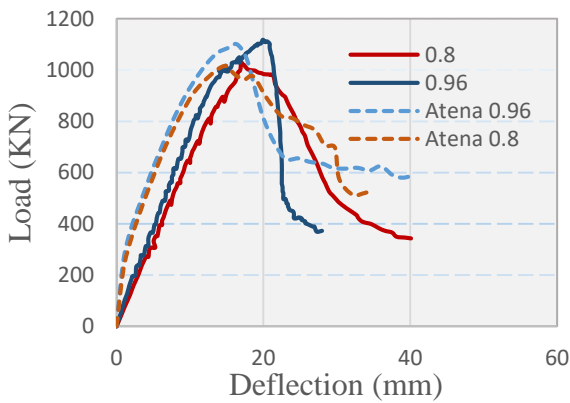


Figure 5. Displays the load-deflection curves of HFRC slab 200mm for Exp. and FE models for HFR200-0.8/0.2 and HFR200-0.96/0.2

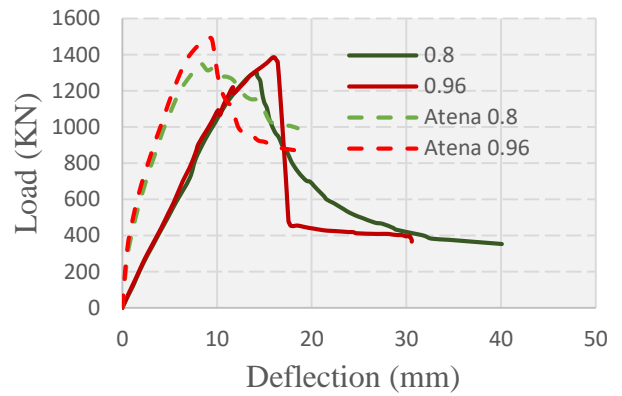


Figure 7. Displays the load-deflection curves of HFRC slab 250mm for Exp. and FE models and HFR250-0.8/0.2 and HFR250-0.96/0.2

Table 4. Displays the results of the ultimate load and deflection with a compressive strength of 50MPa

No.	Specimens name	f_c MPa	Slab thickness mm	$\Delta_{ult.}$ (mm)	$P_{ult.}$ (KN)
1	HFRC-R-0.54			22.80	400.846
2	HFRC-R-0.84			17.83	473.172
3	HFRC-R-1.31			14.87	513.450
4	HFRC-0.68/0.2-0.54			17.87	527.762
5	HFRC-0.68/0.2-0.84	50	150	15.88	547.025
6	HFRC-0.68/0.2-1.31			14.88	586.775
7	HFRC-0.8/0.2-0.54			29.44	547.467
8	HFRC-0.8/0.2-0.84			19.95	557.170
9	HFRC-0.8/0.2-1.31			17.44	590.280
10	HFRC-0.96/0.2-0.54			24.68	563.682
11	HFRC-0.96/0.2-0.84			21.90	606.995
12	HFRC-0.96/0.2-1.31			14.89	623.778
13	HFRC-R-0.4			17.703	670.319
14	HFRC-R-0.63			15.009	819.776
15	HFRC-R-0.98			10.158	842.235
16	HFRC-0.68/0.2-0.4			19.38	875.657
17	HFRC-0.68/0.2-0.63			12.49	903.167
18	HFRC-0.68/0.2-0.98	50	200	9.86	872.899
19	HFRC-0.8/0.2-0.4			16.90	800.999
20	HFRC-0.8/0.2-0.63			12.00	833.803
21	HFRC-0.8/0.2-0.98			11.87	873.434

Table 4. Displays the results of the ultimate load and deflection with a compressive strength of 50MPa (continued)

22	HFRC-0.96/0.2-0.4			19.52	862.374
23	HFRC-0.96/0.2-0.63			14.85	937.483
24	HFRC-0.96/0.2-0.98			11.90	963.232
25	HFRC-R-0.32			13.60	942.254
26	HFRC-R-0.5			11.86	1177.716
27	HFRC-R-0.79			7.94	1275.809
28	HFRC-0.68/0.2-0.32			10.11	1068.399
29	HFRC-0.68/0.2-0.5			7.96	1095.076
30	HFRC-0.68/0.2-0.79	50	250	7.83	1123.725
31	HFRC-0.8/0.2-0.32			11.11	1055.130
32	HFRC-0.8/0.2-0.5			11.52	1129.812
33	HFRC-0.8/0.2-0.79			10.26	1177.635
34	HFRC-0.96/0.2-0.32			15.75	1204.220
35	HFRC-0.96/0.2-0.5			10.57	1234.673
36	HFRC-0.96/0.2-0.79			6.70	1214.562

Table 5. Displays an experimental cracking pattern with a finite element cracking pattern for HFRC slab 200mm and 250mm

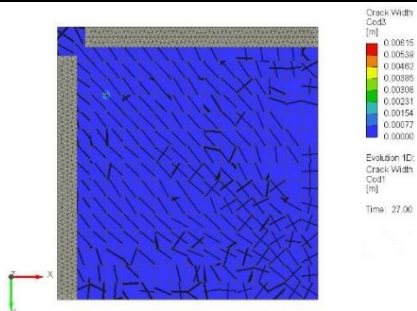
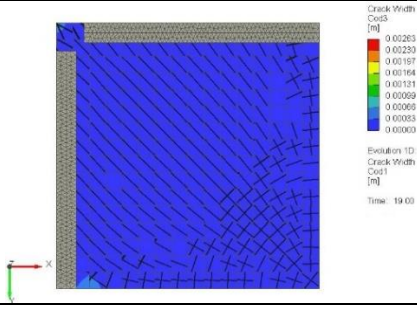
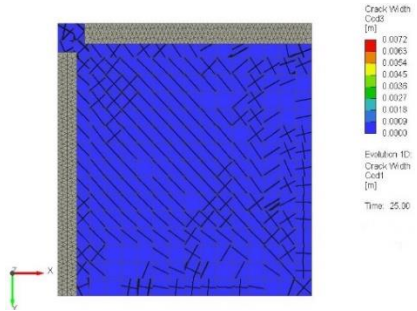
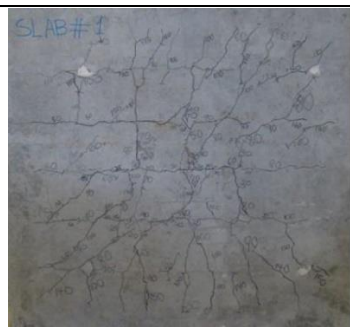
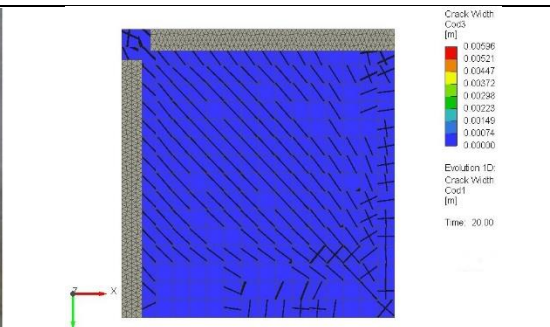
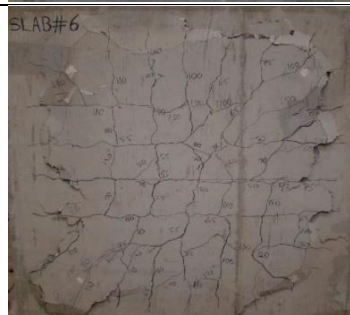
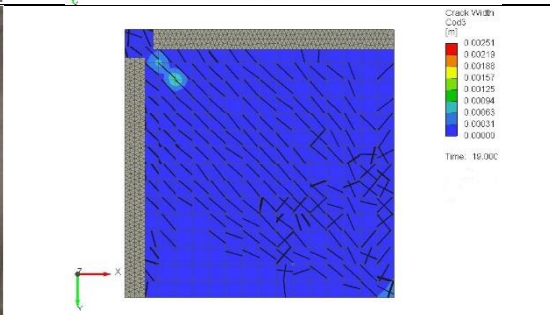
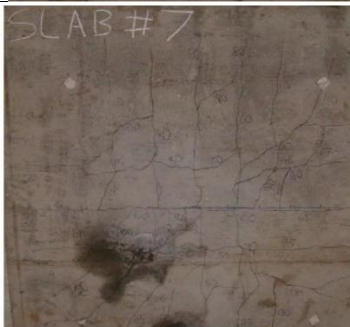
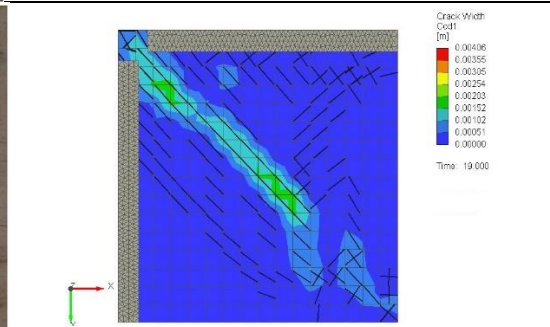
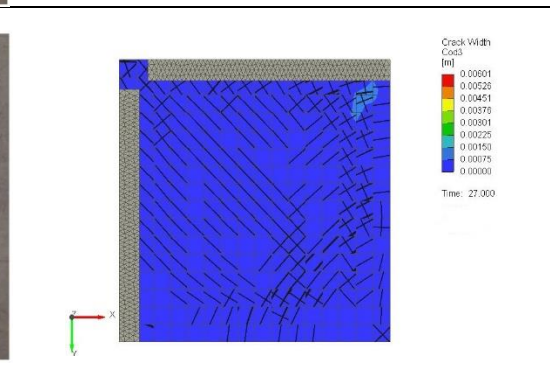
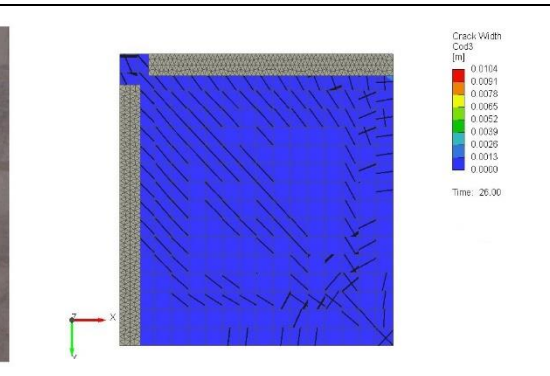
No.	Specimens name	Experimental cracks pattern	Finite Element cracks pattern
1	Reference 200		
2	HFR200-0.68/0.2		
3	HFR200-0.80/0.2		

Table 5. Displays an experimental cracking pattern with a finite element cracking pattern for HFRC slab 200mm and 250mm (continued)

<p>HFR200-0.96/0.2</p>		
<p>Reference 250</p>		
<p>HFR250-0.68/0.2</p>		
<p>HFR250-0.80/0.2</p>		
<p>HFR250-0.96/0.2</p>		

4 Conclusions

The work is focused on examining the effects of hybrid fiber volume fraction on slab depth, and reinforcement ratio, as the main factors, which affect the structural behavior of HFRC two-way slabs. The FE technique was used to understand the behavior of HFRC two-way slabs.

The following are the major conclusions of the parametric study:

The increase in slab thickness from 150 to 200 and 250mm with all reinforcement ratios leads to an increase in the ultimate load and a decrease in the deflection of the HFRC slabs

It has been declared from the results shown in Table 4 that the slab thickness works inversely with the punching shear capacity of the HFRC slab; while the thickness of the slab was increased, the ultimate shear capacity was reduced.

The increase in the reinforcement ratio leads to an increase in the ultimate load and a decrease in deflection for the HFRC slabs.

Also the reinforcement ratio works inversely with the punching shear capacity of the HFRC slab so that increasing the reinforcement ratio decreases the ultimate shear capacity in all slabs.

Conflict of interest

The author declares that there is no conflict of interest.

Similarity rate (iThenticate): 14%

References

- [1] S.A. Al-Ta'an and A.A. Abdul-Razzak, Geometrical and material nonlinear finite analysis of fiber reinforced concrete slabs. IOP Conference Series: Materials Science and Engineering, 2020. <https://dx.doi.org/10.1088/1757-899X/978/1/012041>
- [2] Mabrouk, R.T. and A.A. Hegab. Analysis of the punching behavior of RC flat slabs with horizontal and vertical shear reinforcement. MATEC Web Conf. 120 010062017. <https://doi.org/10.1051/mateconf/201712001006>
- [3] J.A.O. Barros, B.N.M. Neto, G.S.S.A. Melo, C.M.V. Frazão, Assessment of the effectiveness of steel fibre reinforcement for the punching resistance of flat slabs by experimental research and design approach. Composites Part B: Engineering, 78, 8-25, 2015. <https://doi.org/10.1016/j.compositesb.2015.03.050>
- [4] A.H. Aziz and S.S. Kareem, Development, Experimental study for punching shear behavior in RC flat plate with hybrid high strength concrete. Journal of Engineering and Sustainable Development, 17(3), 105-119, 2013.
- [5] R. Koppitz, A. Kenel and T. Keller, Punching shear of RC flat slabs—review of analytical models for new and strengthening of existing slabs, Engineering Structures, 52, 123-130, 2013. <https://doi.org/10.1016/j.engstruct.2013.02.014>
- [6] M.S. Bharath and M.L. Pothula, Experimental study on punching shear strength of fiber reinforced hvfa concrete slabs. International Journal of Scientific Engineering and Technology Research, 05(36), 7579-7586, 2016.
- [7] W.A. Labib, Evaluation of hybrid fibre-reinforced concrete slabs in terms of punching shear. Construction and Building Materials, 260, 119763, 2020. <https://doi.org/10.1016/j.conbuildmat.2020.119763>
- [8] T.H. Almusallam, A.A. Abadel, Y.A. A.N. A. Siddiqui and H. Abbas, Effectiveness of hybrid-fibers in improving the impact resistance of RC slabs. International Journal of Impact Engineering, 81, 61-73, 2015. <https://doi.org/10.1016/j.ijimpeng.2015.03.010>
- [9] K. Kobayashi and R. Cho, Flexural characteristics of steel fibre and polyethylene fibre hybrid-reinforced concrete. Composites, 13(2), 164-168, 1982. [https://doi.org/10.1016/0010-4361\(82\)90054-4](https://doi.org/10.1016/0010-4361(82)90054-4)
- [10] F. Sermet and A. Ozdemir, Investigation of punching behaviour of steel and polypropylene fibre reinforced concrete slabs under normal load. Procedia Engineering, 161, 458-465, 2016. <https://doi.org/10.1016/j.proeng.2016.08.590>
- [11] S. P. Shah, J.I. Daniel, S. H. Ahmad, M. Arockiasamy, P. N. Balaguru, C. G. Ball and R.F. Zollo, Guide for specifying, proportioning, mixing, placing, and finishing steel fiber reinforced concrete. ACI Materials Journal, 90(1), 94-101, 1993.
- [12] P. Pujadas, A. Blanco, S.H.P. Cavalaro, A. Fuente and A. Aguado, Flat suspended slabs reinforced only with macro-synthetic fibres. In Proceedings of the 9th RILEM International Symposium on Fiber Reinforced Concrete (BEFIB 2016), Vancouver, BC, Canada, 19–21 September 2016.
- [13] ACI 544.1R-96, report on fiber reinforced concrete. American Concrete Institute, Farmington Hills, Michigan, USA, 1996.
- [14] S. Kinnunen and H. Nylander, Punching of concrete slabs without shear reinforcement. Elander Boktryckeri Aktiebolag, Sweden, 1960.
- [15] ZP Bazant and Z Cao, Size effect in punching shear failure of slabs. ACI Structural Journal, 84(1), 44-53, 1987.
- [16] A Caratelli, S Imperatore, A Meda, Z Rinaldi, Punching shear behavior of lightweight fiber reinforced concrete slabs. Composites Part B: Engineering, 99, 257-265, 2016. <https://doi.org/10.1016/j.compositesb.2016.06.045>
- [17] R. Pourreza, Investigating the effects of hybrid fibres on the structural behaviour of two-way slabs. PhD Thesis. Memorial University of Newfoundland, 2014.
- [18] M. AlHamaydeh and M.A. Orabi, Punching shear behavior of synthetic fiber-reinforced self-consolidating concrete flat slabs with GFRP bars. Journal of Composites for Construction, 25(4), 04021029, 2021. [https://doi.org/10.1061/\(ASCE\)CC.19435614.0001131](https://doi.org/10.1061/(ASCE)CC.19435614.0001131)
- [19] E.K. Sayhood, S.P. Yaakoub and H.F. Hussien, Nonlinear finite element analysis for punching shear resistance of steel fibers high strength reinforced

- concrete slabs. *Jour. of Engineering and Technology*, 32(6), 1411-1432, 2014.
- [20] M. Navarro, S. Ivorra and F.B. Varona, Parametric finite element analysis of punching shear behaviour of RC slabs reinforced with bolts. *Computers & Structures*, 228, 106147, 2020. <https://doi.org/10.1016/j.compstruc.2019.106147>
- [21] V. Cervenka, J. Cervenka, Z. Janda, D. Pryl, ATENA Program Documentation, Part 8: User's Manual For Atena-Gid Interface; Cervenka Consulting, Prague, Czech Republic, 2017.
- [22] M.S. Al Jawahery, M.E. Gulsan, H.M. Albegmpri, I.A.H. Mansoori and A. Cevik Experimental investigation of rehabilitated RC haunched beams via CFRP with 3D-FE modeling analysis. *Engineering Structures*, 196, 109301, 2019. <https://doi.org/10.1016/j.engstruct.2019.109301>
- [23] V. Cervenka, L. Jedele and J. Cervenka, ATENA Program Documentation. Theory And User Manual, Cervenka Consulting, Czech Republic, Prague, 2018.
- [24] M.S. Al Jawahery, A. Cevik and M.E. Gulsan, 3D FE modeling and parametric analysis of steel fiber reinforced concrete haunched beams. *Advances in Concrete Construction*. 13(1), 45-69, 2022. <https://doi.org/10.12989/acc.2022.13.1.045>

